

**Estimation of the EGR rate in a GDI
engine working in stratified mode using
the ionization current**

Mattias Bruce

LiTH-ISY-EX-3083

December 12, 2000

**Estimation of the EGR rate in a GDI
engine working in stratified mode using
the ionization current**

Examensarbete utfört i Fordonssystem
vid Tekniska Högskolan i Linköping
av

Mattias Bruce

Reg nr: LiTH-ISY-EX-3083

Supervisor: **Dr. Martin Hart, DaimlerChrysler**
Eva Finkeldei, DaimlerChrysler

Examiner: **Prof. Lars Nielsen**

Linköping, December 12, 2000.

	Avdelning, Institution Division, Department Vehicular Systems Dept. of Electrical Engineering		Datum: Date: December 12, 2000
	Språk Language <input type="checkbox"/> Svenska/Swedish <input checked="" type="checkbox"/> Engelska/English <input type="checkbox"/> _____	Rapporttyp Report category <input type="checkbox"/> Licentiatavhandling <input checked="" type="checkbox"/> Examensarbete <input type="checkbox"/> C-uppsats <input type="checkbox"/> D-uppsats <input type="checkbox"/> Övrig rapport <input type="checkbox"/> _____	ISBN ISRN Serietitel och serienummer ISSN Title of series, numbering LITH-ISY-EX-3083
URL för elektronisk version http://www.fs.isy.liu.se			
Titel: Uppskattning av mängd EGR i en GDI motor arbetandes i stratifierad mod genom jonströmmen Title: Estimation of the EGR rate in a GDI engine working in stratified mode using the ionization current Författare: Mattias Bruce Author:			
Sammanfattning Abstract <p>The goal of this thesis is to get a feedback from the cylinder of the amount of Exhaust Gas Recirculation (EGR) being used. To get the feedback the in-cylinder measurement technique of measuring the ionization current is used. The ion current signal is analyzed to extract the information about the amount of exhaust gas in the cylinder.</p> <p>Two basically different methods are used for estimating the EGR rate. The first method is based only on general knowledge of how the EGR rate affects the ion current signal. The second method is based upon the physics of the combustion process.</p> <p>In the first method two different filters are tested, a static Kalman filter and a dynamic Kalman filter. The first filter produces the best results. With this filter an accurate estimation of the EGR rate is reached within 40 cycles. The dynamic filter is developed in an attempt to get a faster estimation. But using this filter no acceptable results are reached. The faster estimation makes it so that the output never stabilizes on one value.</p> <p>For the physically based approach the speed of the flame and the speed with which the flame kernel expands through the cylinder are studied. It is shown that the laminar burning speed of the flame would prove to be a good way of estimating the EGR rate if a physical connection between the ionization signal and the laminar burning speed of the flame speed could be found. No such connection is found in this thesis and thus no estimation of the EGR rate can be made using this method.</p>			
Nyckelord Keywords Ionization current, Exhaust Gas Recirculation, Kalman filter, Sensitivity			

Abstract

The goal of this thesis is to get a feedback from the cylinder of the amount of Exhaust Gas Recirculation (EGR) being used. To get the feedback the in-cylinder measurement technique of measuring the ionization current is used. The ion current signal is analyzed to extract the information about the amount of exhaust gas in the cylinder.

Two basically different methods are used for estimating the EGR rate. The first method is based only on general knowledge of how the EGR rate affects the ion current signal. The second method is based upon the physics of the combustion process.

In the first method two different filters are tested, a static Kalman filter and a dynamic Kalman filter. The first filter produces the best results. With this filter an accurate estimation of the EGR rate is reached within 40 cycles. The dynamic filter is developed in an attempt to get a faster estimation. But using this filter no acceptable results are reached. The faster estimation makes it so that the output never stabilizes on one value.

For the physically based approach the speed of the flame and the speed with which the flame kernel expands through the cylinder are studied. It is shown that the laminar burning speed of the flame would prove to be a good way of estimating the EGR rate if a physical connection between the ionization signal and the laminar burning speed of the flame speed could be found. No such connection is found in this thesis and thus no estimation of the EGR rate can be made using this method.

Keywords: Ionization current, Exhaust Gas Recirculation, Kalman filter, Sensitivity

Acknowledgments

This work has been done for DaimlerChrysler AG in Stuttgart. I would like to thank my supervisors Martin Hart and Eva Finkeldei for their help and support. Special thanks to Christoph Arndt for his help on the filtering and to Rüdiger Herweg and Michael Kessler for their help with the physics of the ion current signal and the combustion process.

I would also like to thank all the people working at the engine team for making my stay in Germany as pleasant as it has been.

Esslingen, December 2000

Mattias Bruce

Notation

Symbols

Θ	Crank angle
I	Ion current
σ	Variance
μ	Mean value
ρ	Correlation and density
λ	Normalized air/fuel ratio
ϕ	Normalized fuel/air ratio ($\phi = \lambda^{-1}$)
S_L	Laminar burning speed
S_t	Turbulent burning speed
r_K	Flame kernel radius
p	Pressure
T	Temperature
V	Volume
A	Area
m	Mass
u'	Turbulence intensity
\bar{U}	Mean flow velocity
L	Integral length scale
I_0	Strain factor
B	Cylinder bore
l	Connecting rod length
a	Crank radius
γ	Ratio of specific heats

Abbreviations

EGR	Exhaust Gas Recirculation
GDI	Gasoline Direct Injection
ECU	Electronic Control Unit
rpm	Rounds Per Minute (engine speed)
PFI	Port Fuel Injection
TDC	Top Dead Center

Contents

1	Introduction	1
1.1	Background	1
1.2	Methods	2
1.3	Thesis outline	2
2	The engine	3
2.1	Gasoline Direct Injection (GDI)	3
2.2	Exhaust Gas Recirculation (EGR)	4
2.3	Measurements	5
3	Internal combustion	7
3.1	The combustion process	7
3.2	Ion generation	8
3.3	Effects of EGR on the combustion and ion current	11
4	EGR rate estimation using filters	13
4.1	Static Kalman filter	13
4.2	Dynamic Kalman filter	17
5	Physically based EGR rate estimation	23
5.1	Laminar burning speed	23
5.2	Sensitivity	23
5.3	Flame kernel radius	26
5.4	EGR estimation	30
6	Conclusions	31
	References	34
	Appendix A: Derivation of the sensitivity formula S_{λ}^{SL}	35

List of Figures

2.1	The different placements of the injector in (a) a port-injected engine and (b) a GDI engine.	3
2.2	A schematic layout of the EGR system.	5
3.1	Typical form of the ion current signal.	8
3.2	Effects of EGR on the ion current.	11

4.1	Correlation between the EGR rate and (a) amplitude of the first maximum, (b) position of first maximum, (c) area under the first maximum.	13
4.2	A flowchart of the algorithm using the static Kalman filter.	14
4.3	Output from the static Kalman filter.	16
4.4	Correlation between the EGR rate and (a) the mean value, (b) the amplitude of the first maximum.	18
4.5	A flowchart of the algorithm using the dynamic Kalman filter.	20
4.6	Output from the dynamic Kalman filter.	21
5.1	Sensitivity of the laminar burning speed to λ and EGR rate.	25
5.2	Effects on the laminar burning speed of different EGR rates and λ values.	25
5.3	The flame kernel radius and the ion current signal plotted for different EGR rates.	29
5.4	The kernel radius at the position of the first maximum for different EGR rates.	29

List of Tables

3.1	Ionization energy for the most important species found in the post-flame zone.	10
3.2	The most important electronegative species in the post-flame zone, the value for water is a bit uncertain.	10

1 Introduction

The goal of this thesis is to try to estimate the Exhaust Gas Recirculation (EGR) rate using the ion current signal. The main advantage of the ion current is that no extra sensor equipment needs to be added to the engine which makes the method very cheap. The disadvantages are that the signal is noisy, has a low signal level, contains very large cycle-to-cycle variations and it is only a local measurement around the spark plug. Another problem is the lack of analytical expressions of how the amount of EGR affects the combustion and thus the ion current.

The work has been done with measurement data from a GDI engine working in stratified mode (see section 2.1) with EGR rates between 0 and 25%.

1.1 Background

The regulations and laws on the amount of emissions let out by modern vehicles gets stricter and stricter all the time. To be able to cope with these new laws the car industry needs to develop new methods for lowering fuel consumption and emissions. One such method is to recirculate some of the exhaust gas back into the cylinder. This is an effective way to lower the peak temperatures in the cylinder and thus lowering the amount of NO_x created. A higher EGR rate gives a better engine performance in aspect to the amount of emissions let out, but too much EGR gives an unstable combustion which sets a limit on how much EGR that can be used.

Today there exists no good way of determining exactly how much EGR that is used which sets a low limit on how much EGR that can in fact be used. This is because the car producers need to make sure that they don't use too much as this would cause the engine to stop due to failure of igniting the air-fuel mixture. To do this they keep the EGR rate far away from the limit, typically an engine can handle that up to 25% of the inlet air consists of recycled gas but today seldom more than 15% is used. The control of the amount of EGR is done by using maps that control the EGR valve based on the engine speed and load.

The ion current is already used in production cars for knock sensing, detection of missfire and for cam phase sensing [1]. It has also been shown that it can be used for ignition control [2, 3, 4] and work has been done to determine the air/fuel ratio in the cylinder from the signal [5].

1.2 Methods

In this thesis two basically different methods to estimate the EGR rate are investigated.

The first method is based on knowledge of how the EGR rate affects the ionization signal in general. From this knowledge certain features of the signal are selected. These features and the use of two different Kalman filters give two ways of estimating the EGR rate. One is that from each feature an EGR rate was calculated and then a static filter is used to weight these features together to an estimate. In the second algorithm the features are used in a dynamic Kalman filter to get the estimation of the EGR rate.

The second method is an attempt to find an analytical way of calculating the EGR rate from the ionization signal. To do this the flame speed and the early development of the flame kernel are studied.

1.3 Thesis outline

The work done during this thesis and the concepts contained in the thesis are described in the following chapters.

Chapter 2, The Engine. An overview of how the GDI engine works in its two different operating modes and an explanation of the EGR system.

Chapter 3, Internal Combustion. An introduction to the processes taking place in the cylinder during the combustion. The general shape of the ionization signal is discussed and the effects upon this signal and the combustion in general by the EGR rate are explained.

Chapter 4, EGR rate estimation using filters. The two different algorithms used to estimate the EGR rate are explained. The differences between the algorithms and the Kalman filters used in them are shown and the results discussed.

Chapter 5, Physically based EGR rate estimation. The models and formulas for the kernel development and the flame speed are studied to see if they can be a good way to estimate the EGR rate.

Chapter 6, Conclusions The conclusions that are drawn from this work are presented in this chapter.

2 The engine

The engine that the measurements used in this master thesis come from is a one-cylinder engine. The engine uses the gasoline direct injection system and exhaust gas recirculation.

The main idea behind the GDI engine is to combine the high power output of an Otto engine with the good fuel economy of the diesel engine. The reason for the EGR system is to reduce the formation of NO_x pollutants. For a complete description of Otto and diesel engine operation see Heywood [6].

2.1 Gasoline Direct Injection (GDI)

The concept of the gasoline direct injection engine dates back to the 1920s but only during the last decade working engines with any benefits over normal engines have started to appear. Still today there are few good GDI engines on the market but most major engine manufacturers are developing their own GDI engines.

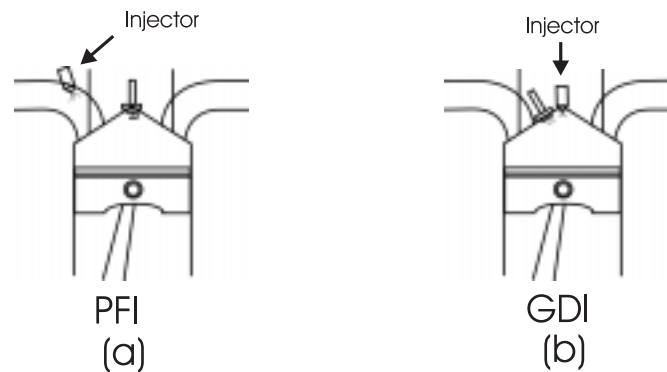


Figure 2.1: The different placements of the injector in (a) a port-injected engine and (b) a GDI engine.

In a direct injection engine the fuel is injected directly into the cylinder and not like on most modern cars into the inlet pipe just before the cylinder, as is shown in figure 2.1. By separating the air intake from the fuel injection a number of advantages can be obtained while using the engine at part load.

- Unthrottled operation: By controlling the fuel separately from the air the throttle can be removed and thus reducing the pump losses in the

engine.

- Increased volumetric efficiency: The vaporization of the fuel in the cylinder reduces the temperature and this can increase the volumetric efficiency with up to 10% [7].
- Reduced knock tendency: The lower temperature and the late injection reduce the engines knock tendency. This allows the compression ratio to be higher which increases the engines efficiency.
- Ultra-lean mixture ($\lambda \gg 1$): By injecting the fuel late during the compression stroke the injected fuel can be positioned around the spark plug and a volume with $\lambda \cong 1$ is created that can be easily ignited while in the rest of the combustion chamber an ultra-lean mixture is obtained.

There are also drawbacks to this technique. The biggest being that while the ultra-lean combustion is very good for the fuel economy it has the effect that due to the excess air in the exhaust gases a normal three way catalyst is not working for NO_x reduction. This means that an additional NO_x catalyst/trap must be used. Also the particle emissions from the engine will be higher than those of a port injected engine. When the GDI engine is working like this it is said to work in the stratified mixture mode. In stratified mode a GDI engine has about 15% better fuel economy than a port injected engine [7]. This is mostly due to the reduced pumping losses.

To achieve the same maximal energy output as from a port injected engine the GDI engine will switch operating mode to the homogeneous mixture preparation at high engine loads. In this mode the fuel is injected during the intake stroke and then have enough time to mix with the air so that an homogeneous mixture with $\lambda = 1$ is achieved. Still the GDI engine retains the advantages of increased volumetric efficiency and reduced knock tendency.

2.2 Exhaust Gas Recirculation (EGR)

The troubles mentioned above with the high NO_x emissions in stratified mode makes it necessary to use other ways than the normal three way catalyst to reduce the NO_x emissions. One effective way is to use EGR. By recirculating some of the exhaust gas the peak temperature of the combustion is lowered leading to a heavily reduced formation of NO_x .

The drawback with the EGR is that if too much is used it reduces the stability of the combustion. This sets a limit on how much EGR the engine

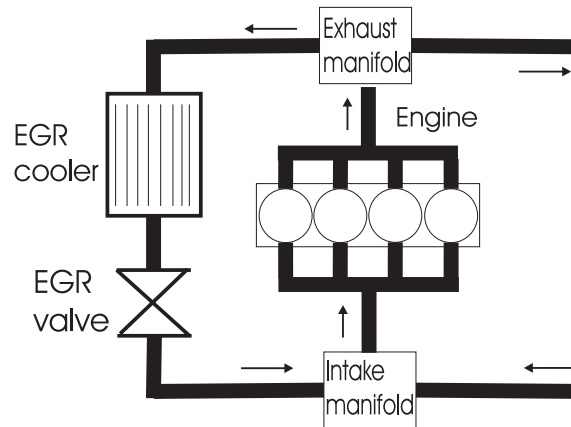


Figure 2.2: A schematic layout of the EGR system.

can use. For normal engines this is about 25%, but on GDI engines working in stratified mode it has been reported that it is possible to use up to 50% EGR [8]. If the amount of exhaust gas rises above this limit it is no longer possible to ignite and burn the mixture in the chamber.

Figure 2.2 shows a principal drawing of how the EGR system works. Part of the exhaust gas is taken from the exhaust manifold and then cooled before it is let into the intake pipe just before the intake manifold. In the manifold the exhaust gas and the fresh air mixes to a homogeneous mixture that is then sucked into the cylinder. The EGR rate is then defined as the percentage of the mixture that enters the cylinder that is recirculated gas. This rate is controlled by using the EGR valve. For the system to work the exhaust pipe must have a slightly higher pressure than the inlet pipe so that the exhaust gas is sucked into the inlet.

2.3 Measurements

No measurements have been done during this thesis work, instead measurements made earlier have been used. A brief explanation of the measurement systems for the ion current and the EGR rate are given though.

For measuring the ionization in the cylinder an electrical field is created by applying an AC-voltage to the spark plug. The electrical field gets the ions and electrons moving towards their corresponding electrode. This creates a current that is measured. A detailed explanation of the ion measurement system can be found in [9].

To measure the EGR rate a comparison between the *CO*-massflow on the intake and the exhaust sides of the engine is made. From the difference in the flows the EGR rate is calculated. This requires that the engine is held at static operating conditions as the analysis of the gases takes some time. The accuracy in this measurement is an absolute value of $\pm 2\%$ from the given EGR rate.

3 Internal combustion

In an internal combustion engine the chemical energy in the fuel is converted to mechanical energy in the engine. This is achieved by igniting a mixture of air and fuel and letting the resulting expansion of the gases push a piston.

3.1 The combustion process

Both diesel and gasoline engines work according to the four stroke principle. The strokes being

Intake. The mixture of air and recirculated gas is sucked into the cylinder.

In a port injected engines the fuel is also sucked in during this stroke and in GDI engines working in homogeneous mode the fuel is injected during this phase.

Compression. The mixture is compressed raising the temperature and pressure in the cylinder. For a GDI engine working in stratified mode the fuel is injected during the compression stroke. The injection is timed so that at the ignition time (around 25° before TDC) an area with $\lambda \cong 1$ is created around the spark plug. The ignition starts the combustion that continues into the expansion phase.

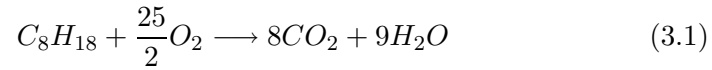
Expansion. The expansion of the burning gases increases the pressure in the cylinder creating a force that pushes the piston downwards. The combustion stops when the flame reaches the chamber walls and is quenched.

Exhaust. Finally the burned gas is pushed out of the cylinder and a new cycle can begin.

For this work only the early stages of the combustion are of interest. The combustion is started by the ignition system with the use of the spark plug. An electrical discharge of the ignition system creates a breakdown of the gas in the spark plug gap. During the breakdown the gas is converted into an electrically conducting plasma channel that ignites the air-fuel mixture [10]. The ignition creates a small flame kernel that then expands out through the cylinder leaving the hot burned gases behind.

The reactions that take place within the flame are very complex, in a simplified model the hydrocarbons in the fuel react with the oxygen in the air forming carbon-dioxide and water. For isooctane the chemical reaction

that takes place is



But many other chemical reactions are taking place at the same time. The reactions that produces the ions are studied in more detail to get an understanding of how the ion current signal is created and what affects it.

3.2 Ion generation

The ionization signal has three clearly defined phases. First comes the coil ringing in the ignition system that creates a heavily oscillating signal. Second comes the flame front phase and last the post flame phase. During the coil ringing no information about what is happening in the cylinder can be obtained so this part of the signal is not investigated. In figure 3.1 the general form of the ion current signal for the last two phases can be seen.

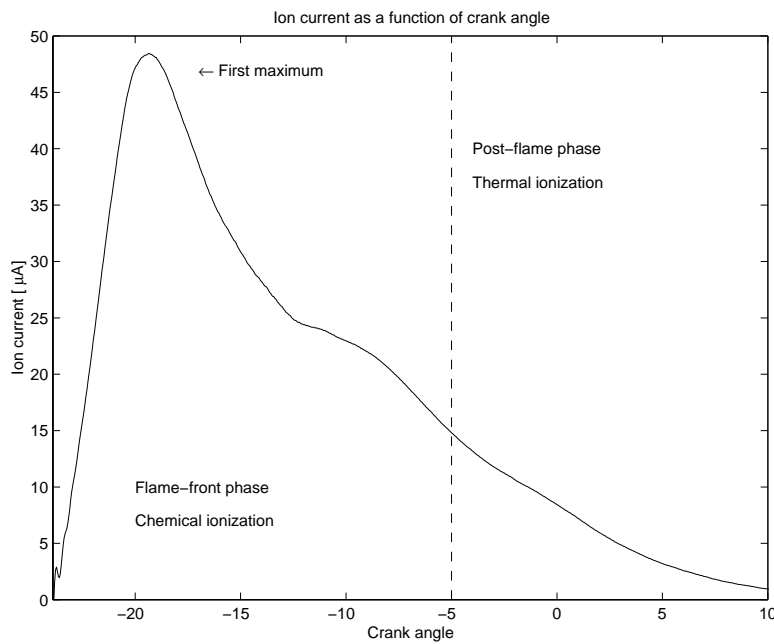


Figure 3.1: Typical form of the ion current signal.

The second part of the signal, the flame front phase, is dependent on the amount of ions in the reaction zone of the flame. This phenomenon was

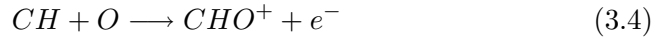
studied in detail by Calcote in the late fifties. He found that the ionization was strongly dependent on the chemistry of the combustion process [11] so it was given the name Chemi-ionization. The process can be described generally by



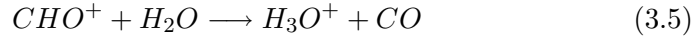
The energy that is available for the ionization is the heat of the reaction ΔH and the activation energy E . The activation energy is the energy that is necessary for the reaction $A+B \rightarrow C+D$ to take place, during this reaction the energy ΔH is released. The energy required for the ionization to take place is V_i . For the reaction to end up in the ionized state the following requirement must then be met.

$$V_i \leq \Delta H + E \quad (3.3)$$

Chemi-ionization thus occurs during an elementary reaction when the activation energy together with the released energy is large enough to ionize one of the reactants. The most significant reaction that follows this requirement has been claimed to be [12]



However, other studies have claimed that H_3O^+ is the dominant ion in the reaction zone. This ion is created by the following reaction



Reaction (3.5) is much faster than reaction (3.4) which is the reason that H_3O^+ -ions are much more common than the CHO^+ -ions as these ions are destructed faster than they are created.

The removal of the H_3O^+ ion is obtained by the dissociative recombination with an electron to form water and hydrogen



The last part of the ion signal, the post-flame phase in figure 3.1, describes the amount of ions after the flame front have passed. In this phase the dominant ionization is the thermal ionization due to the temperature of the gas. The thermal ionization can be regarded as a chemical reaction including only one reactant according to



The energy needed for this reaction is taken from the heat of the burned gas. Studies have claimed that NO is responsible for a very large part of the ions in the post-flame phase [13]. This is due to the low ionization energy of that species, as can be seen in table 3.1. The table also shows the ionization energies for the other major species present in the post-flame zone.

Species	Ionization energy (eV)
NO	9.26405
H_2O_2	10.54
CO	14.0139
CO_2	13.777
H_2O	12.6188
N_2	15.5808
H_2	15.42589

Table 3.1: Ionization energy for the most important species found in the post-flame zone.

The shape of the ion current signal in the post-flame phase is also affected by the formation of negative ions. These ions are formed when species that have a certain affinity for electrons, called electronegative species, attach electrons. The effect on the ion current is that it is lowered due to the lower mobility of the negative ions compared to the electrons. Table 3.2 shows the major electronegative species present in the post-flame zone. In the table it can be seen that oxygen atoms have a high affinity for electrons. The value for water is a bit uncertain.

Species	Electron Affinity (eV)
O	1.4611103
O_2	0.451
N	0.05
H	0.754209
OH	1.82767
H_2O	0.9?
HO_2	1.078

Table 3.2: The most important electronegative species in the post-flame zone, the value for water is a bit uncertain.

In a GDI engine working in stratified mode there is a high amount of excess air. The oxygen in the air will then attach a lot of electrons to it reducing the ion current. This in combination with the lower temperature are the reasons that the post-flame phase of the ion current signal for the stratified mode lacks the typical second maximum that can be seen in the signal from engines with a homogeneous mixture.

3.3 Effects of EGR on the combustion and ion current

The introduction of the nonreactive exhaust gas into the cylinder affects the combustion and thus the ion current. In figure 3.2 the effect that different EGR rates have on the ion current signal can be seen. In the figure there are two lines for each EGR rate between 0% and 25% in steps of 5%. Each line is the average of 120 cycles. The 0% EGR has the highest amplitude and the earliest position of the first maximum.

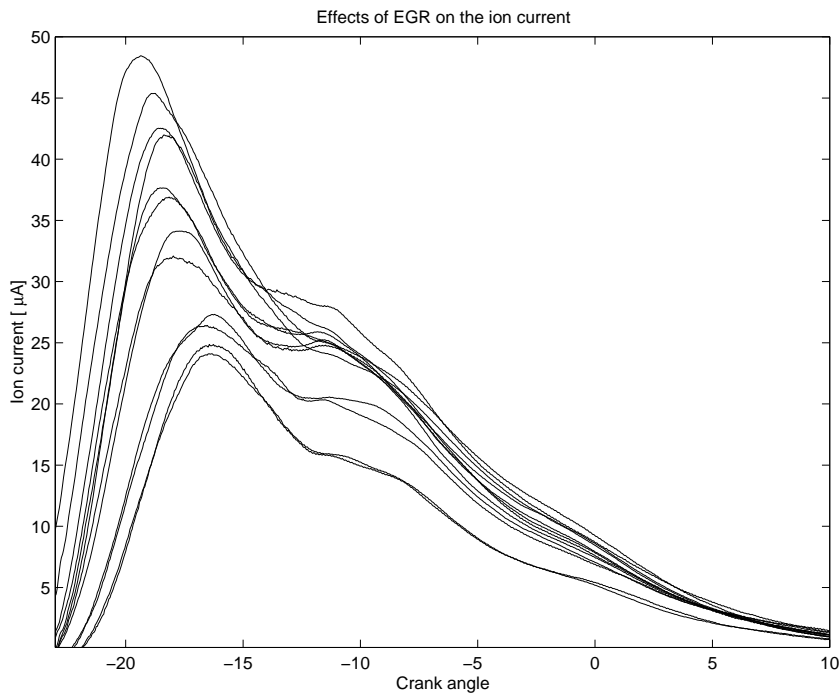


Figure 3.2: Effects of EGR on the ion current.

As have been stated earlier the main reason to use the EGR system is

that it reduces the formation of NO_x in the engine. This is due to that the exhaust gas lowers the peak temperature in the cylinder. The lower temperature is because that the exhaust gas increases the heat capacity ratio κ which means that more energy is needed to raise the temperature of the gas.

With lower amounts of NO in the post-flame zone it can be assumed that the ion current should also be lower in the post-flame zone for higher EGR rates. But as seen in figure 3.2 this is not the case, the reason for this is that the introduction of the exhaust gases also lowers the amount of excess air in the cylinder. This means that there are less O atoms that can attach electrons and lower the ion current. So the lower amount of positive ions are balanced by the lower amount of negative ions. First at very high EGR rates the expected effect on the signal can be seen. The conclusion of this is that the last part of the ion current signal can not be used to get any information about the amount of exhaust gas in the cylinder.

The only possibility that is left for estimating the EGR rate from the ion current signal is thus by looking at the second part of the signal, the flame-front phase. In figure 3.2 it can be seen that the effect of EGR in this phase is a lower amplitude and a later positioning of the first maximum. The total amount of created ions is also lowered as can be seen by studying the area under the maximum.

The lower amplitude and lower amount of ions is expected mainly due to the decreased temperature which reduces the available energy ΔH from equation 3.3. This means that less reactions will fulfill the requirements for formation of ions leading to that less ions are formed. Another reason for the lowered amplitude is that the rates of recombination of the ions aren't affected as much as the production of the ions.

The positioning is affected by the time it takes for the flame to leave the vicinity of the spark plug where the measurement is made. As can be seen in figure 3.2 the first maximum occurs later for higher EGR rates. This effect is also due to the lowered temperature as it leads to a lower burning speed of the flame which in turn gives a slower flame kernel formation.

4 EGR rate estimation using filters

The first method of estimating the EGR rate is to use the general knowledge of the signal gained in the previous chapter. The features of the signal (e.g amplitude of the first maximum) are calculated and used in conjunction with two different kinds of Kalman filters to get an EGR rate estimation.

The first algorithm developed uses a static Kalman filter and the second a dynamic Kalman filter based upon a model of how the EGR rate changes. A Kalman filter is a *Recursive data processing algorithm* and more general information about this kind of filters can be found in for example [14]

4.1 Static Kalman filter

A filter developed for another GDI engine working in stratified mode [15] was used. This filter was modified partly and could thereafter be used with data from the new engine. For this filter three features were selected

- The amplitude of the first maximum.
- The position of the first maximum.
- The area under the first maximum.

The correlation between these three features, calculated in the same way as they are done in the filter algorithm, and the EGR rate is quite good as can be seen in figure 4.1.

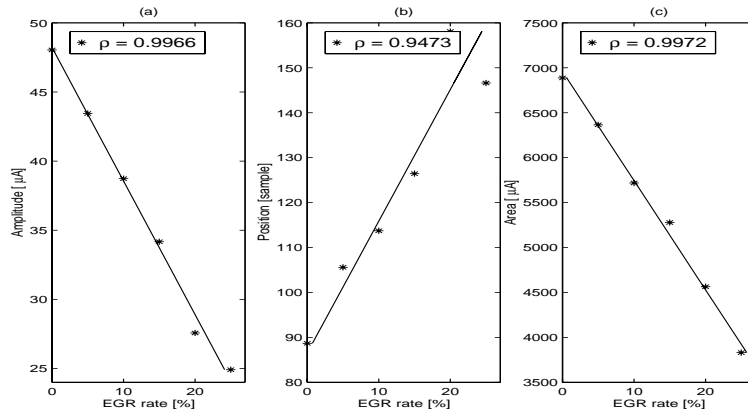


Figure 4.1: Correlation between the EGR rate and (a) amplitude of the first maximum, (b) position of first maximum, (c) area under the first maximum.

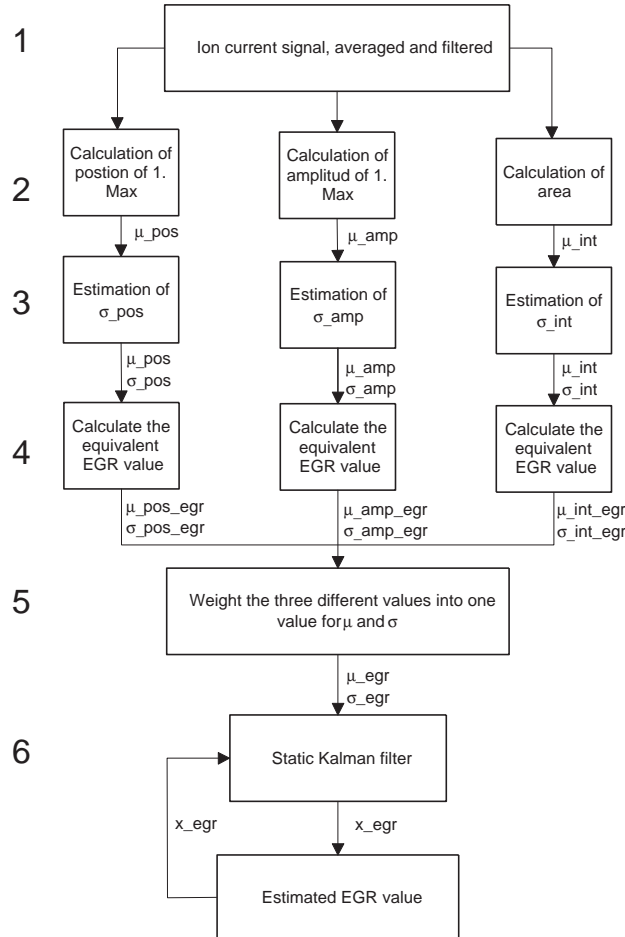


Figure 4.2: A flowchart of the algorithm using the static Kalman filter.

A flowchart of the filter can be seen in figure 4.2, and the different steps of the filter are explained below. In the algorithm it is assumed that the features follow a normal distribution with a certain mean value and variance for each EGR rate.

1. The signal is averaged using a moving average over 6 cycles. This averaged signal is then filtered using a third order zero-phase Butterworth lowpass filter with a 3dB cut-off frequency of 5kHz [16].
2. From the averaged and filtered signal the position and amplitude of the first maximum and the area under the first maximum are calculated.

3. The calculated values from the previous step in conjunction with stored mean and variance values for the different features are used to calculate a variance estimate for each feature using

$$\sigma_y = \frac{(\mu_2 - y)^2 \sigma_1 + (\mu_1 - y)^2 \sigma_2}{(\mu_1 - y)^2 + (\mu_2 - y)^2} \quad (4.1)$$

In equation 4.1 μ_1 and μ_2 are the stored mean values for the EGR rates closest to the measurement y , σ_1 and σ_2 are the variances of the respective features and σ_y is the used estimation for the variance.

4. Linear regression

$$g(x) = kx + m \quad (4.2)$$

is used to calculate an equivalent EGR rate from the features. To get the variance into their EGR values Gauss approximation formula is used (which is exact for a linear function)

$$\sigma_{g(x)} = \sigma_x k^2$$

This formula is weighted with the correlation between the feature and the EGR rate yielding the final formula.

$$\sigma_{EGR} = \sigma_I \left(\frac{k}{\rho^2} \right)^2 \quad (4.3)$$

with σ_{EGR} being the variance in EGR rate and σ_I being the variance of the feature. The correlation between the EGR rate and the ion current is the value ρ .

5. The next step is to weight the three different EGR and σ values into two values. This is done with the following formulas.

$$\mu_{\hat{y}} = \frac{\sigma_{y_2}^2 \sigma_{y_3}^2 y_1 + \sigma_{y_1}^2 \sigma_{y_3}^2 y_2 + \sigma_{y_1}^2 \sigma_{y_2}^2 y_3}{\sigma_{y_1}^2 \sigma_{y_2}^2 + \sigma_{y_1}^2 \sigma_{y_3}^2 + \sigma_{y_2}^2 \sigma_{y_3}^2} \quad (4.4)$$

$$\frac{1}{\sigma_{\hat{y}}^2} = \frac{1}{\sigma_{y_1}^2} + \frac{1}{\sigma_{y_2}^2} + \frac{1}{\sigma_{y_3}^2} \quad (4.5)$$

These equations are extensions of the formulas found in [14] for weighting two measurements into one estimate.

6. The last step of the calculation is to use the static kalman filter to weight the new measurement together with the old estimate into a new estimate.

$$\hat{x}_i = \hat{x}_{i-1} + K (\mu_{\hat{y}} - \hat{x}_{i-1}) \quad (4.6)$$

$$K = \frac{\sigma_{\hat{x}_{i-1}}^2}{\sigma_{\hat{x}_{i-1}}^2 + \sigma_{\hat{y}}^2} \quad (4.7)$$

$$\sigma_{\hat{x}_i}^2 = \sigma_{\hat{x}_{i-1}}^2 - K \sigma_{\hat{x}_{i-1}}^2 \quad (4.8)$$

By looking at equation 4.7 it can be seen that a new value with a high variance $\sigma_{\hat{y}}$ will affect the output from the filter a little while a low variance will have a bigger effect on the filter output. The estimated EGR rate will converge towards a value and for every new sample it becomes harder to get big changes in the filter output. This means that the filter has to be reset when the EGR rate is changed.

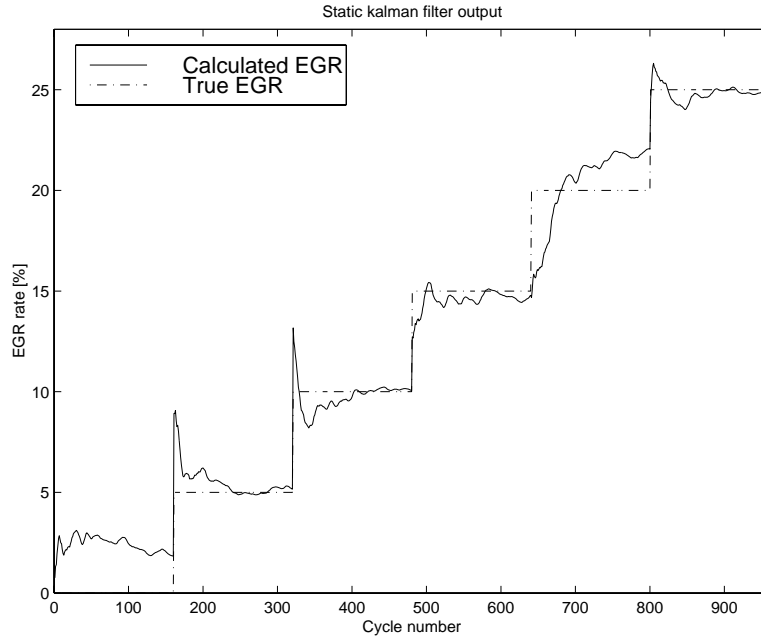


Figure 4.3: Output from the static Kalman filter.

This can be seen in figure 4.3 that shows the output from the filter. In the simulation the EGR rate was constant for 160 cycles and then it was

increased by 5% and at the same time the filter was reset. For all rates except 0% and 20% the result looks good. For all the other EGR rates the result is within 1% (absolute value) from the measured rates after 60 cycles.

One of the reasons for the trouble with the 0% level comes from equation 4.4. A correct y_x value will have a small influence on the $\mu_{\hat{y}}$ value (as it should be small) but if one of the y_x is a big incorrect value it will have a quite big effect on $\mu_{\hat{y}}$. The 0% EGR rate is not that important though as it can easily be found by checking the output from the EGR valve sensor (i.e if the valve is closed there is no external EGR).

For the 20% EGR rate the cycle-to-cycle variations of the signal are the biggest, due to not very stable working conditions during the measurements, which probably is the cause for the bad estimate of this EGR rate.

The filter requires that maps are stored in the ECU containing the mean and variance values, the coefficients for the regressions, the correlation between the features, and the EGR rate at different operating points.

In conclusion the filter have the following advantages and disadvantages.

- Advantages
 - Fast, the calculations used in this filter is straightforward, easy and fast to implement in an ECU.
 - Good estimation, after 30-40 cycles a good estimation of the EGR rate is reached.
- Drawbacks
 - The filter needs to be reset to get to a new EGR value within reasonable time.
 - The signal has to be averaged for the algorithm to be able to produce any results and this slows down the estimation.
 - Sensitive to the initial conditions. If the first few cycles in the estimation is far from the true answer (due to cycle-to-cycle variations) they will affect the filter very much making it so that it takes a longer time before a good estimate is reached.

4.2 Dynamic Kalman filter

In an attempt to get a faster response and to remove the necessity of resetting the filter a dynamic Kalman filter was developed. The algorithm also tested a new method of smoothing the cycle-to-cycle variations of the

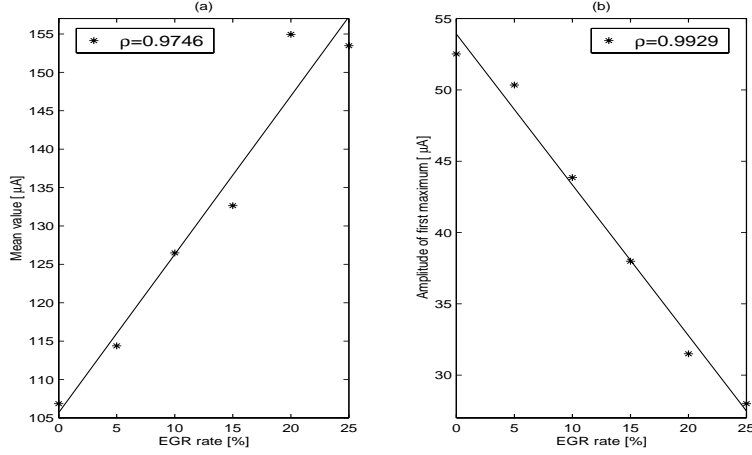


Figure 4.4: Correlation between the EGR rate and (a) the mean value, (b) the amplitude of the first maximum.

signal and a few different features were tried. For the final algorithm the following two features were used.

- The mean value of the first maximum calculated as $\sum(xf(x))$
- The amplitude of the first maximum.

Both these features have a good correlation with the EGR rate as can be seen in figure 4.4. For the amplitude the only difference to the static filter is in the way it is calculated (i.e. smoothing instead of averaging). The reason for using only two features instead of three as in the previous algorithm is that the result did not improve with more features.

For the dynamics of the filter a model over the EGR rate was made using a state-space description. The model has two parts, first the continuous-time system dynamics model from which then the sampled data measurements are taken. In the general form we have

$$\dot{\bar{x}}(t) = F(t)\bar{x}(t) + B(t)\bar{u}(t) + G(t)\bar{w}(t) \quad (4.9)$$

$$\bar{z}(t_i) = H(t)\bar{x}(t_i) + \bar{v}(t_i) \quad (4.10)$$

In this case there is no input signal $\bar{u}(t)$, the state vector \bar{x} consists of two states, the EGR rate and the change in the EGR rate. For the driving noise $\bar{w}(t)$ the difference between the estimated output and the measured output

is used giving the model.

$$\dot{\bar{x}}(t) = \begin{bmatrix} 1 & 1 \\ 0 & 0.9999 \end{bmatrix} \bar{x}(t) + (\bar{z}(t_i) - f(\bar{x})) \quad (4.11)$$

$$\bar{z}(t_i) = H\bar{x}(t_i) + \bar{v}(t_i) \quad (4.12)$$

The value 0.9999 is only used to insure stability in the model. For the state $\bar{x}(t)$, and the two noise signals, the driving noise $\bar{w}(t) = (z(t_i) - f(\bar{x}))$ and the measurement noise $\bar{v}(t)$ the assumption is that they are normal distributions with the following properties

$$\bar{x}(t) \sim N(\hat{x}, P) \quad (4.13)$$

$$\bar{w}(t) \sim N(0, Q) \quad (4.14)$$

$$\bar{v}(t) \sim N(0, R) \quad (4.15)$$

The noise signals are also assumed to have no correlation between to different measurements, so called white noise. These assumptions are important for the working of the dynamic Kalman filter.

A flowchart of the algorithm can be seen in figure 4.5, with a more detailed explanation of the different steps below.

1. The signal is filtered through a third order zero-phase Butterworth low-pass filter with a cut-off frequency of 5 kHz to reduce the noise.
2. The signal is normalized with the area under the first maximum using

$$I_n(\theta) = \frac{I(\theta)}{\sum_{\theta} I(\theta)} \quad \theta_{max} - 5 \leq \theta \leq \theta_{max} + 5 \quad (4.16)$$

with θ_{max} being the position of the first maximum.

3. The mean value and the amplitude of the first max is calculated. For the mean value calculation the normalized signal is used and for the amplitude the filtered signal.
4. Filters are used to smooth the features. These filters work like the dynamic Kalman filter described below with the differences that we only have one state, the feature, and no model describing the change in the feature. This means that a one-dimensional static version of equations 4.17-4.21 is used with $F = H = 1$ and $f(\hat{x}) = \hat{x}$ to do the smoothing. The similarity between this smoothing filter and the static filter used in the previous algorithm should be noticed.

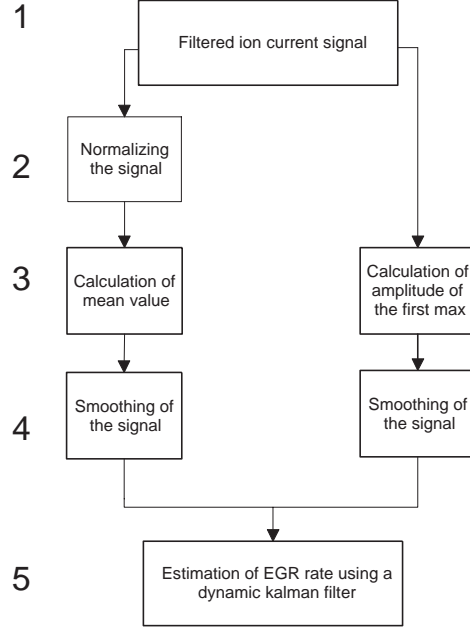


Figure 4.5: A flowchart of the algorithm using the dynamic Kalman filter.

5. The last step is to estimate the EGR rate. This is done in two steps, first the model is used to predict the new EGR value just before the new measurement is made at time t_i^- .

$$\hat{x}_i^- = F\hat{x}_{i-1} \quad (4.17)$$

$$P_i^- = FP_{i-1}F^T + Q \quad (4.18)$$

With \hat{x} and P being the mean value and variance of the state from equation 4.13. The new measurement is then taken at time t_i , this measurement is then finally incorporated in the estimate for time t_i^+

$$K_g = P_i^- H^T [HP_i^- H^T + R]^{-1} \quad (4.19)$$

$$\hat{x}_i^+ = \hat{x}_i^- + K_g (z(t_i) - f(\hat{x}_i^-)) \quad (4.20)$$

$$P_i^+ = P_i^- - K_g H P_i^- \quad (4.21)$$

With \hat{x}_i^+ holding the new estimation of the EGR rate. In these equations K_g is a weighting function for the new measurement that is based upon the variances R , P and Q , through the P^- value, from equations

4.13-4.15. The derivation of these formulas can be found in Maybeck [14].

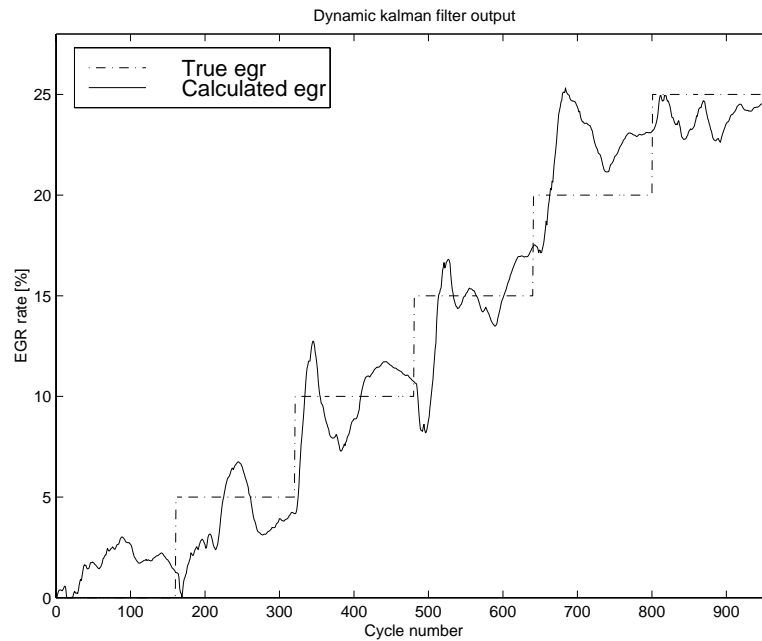


Figure 4.6: Output from the dynamic Kalman filter.

As can be seen in figure 4.6 the output from the filter is not satisfying. The faster response times have been introduced at the cost of the stability of the output. For most EGR rates the estimation is oscillating around the right level but never stabilizes on it.

Like for the static filter it can be seen that the worst result is for the 20% EGR rate which probably also is partly due to the measurements. The main reason for the bad result for the other EGR rates is the fact that no averaging is done on the signal. During the development of the static filter different amounts of averaging was tried and without any averaging no satisfying results could be reached. The result improved the more averaging that was used.

The reason why no averaging is done is that it destroys the assumption made earlier about the white noise. If the signal is averaged we introduce a correlation between different times for the noise giving, especially the

driving noise, an unwanted time dependency which has the effect that the quality of filter output is decreased.

In the view that no averaging is done the output is better than that of the static filter with no averaging. It should also be noticed that all the measurements used during this thesis work is for static operating conditions of the engine. If an estimation of the EGR rate during dynamic operation is wanted the static filter can not be used and then the dynamic filter might prove useful.

5 Physically based EGR rate estimation

In an attempt to find a physical based formula describing the connection between the ion current and the EGR rate the speed of the flame in the cylinder and the development of the flame kernel are studied.

5.1 Laminar burning speed

The laminar burning speed is used since that it is the only equation describing the combustion process found that includes the EGR rate as an variable.

From[6] the equation for the laminar burning speed of the flame was taken

$$S_L = S_{L,0} \left(\frac{T_u}{T_0} \right)^\alpha \left(\frac{p}{p_0} \right)^\beta \left(1 - 2.06F^{0.77} \right) \quad (5.1)$$

In the formula $T_0 = 298K$ and $p_0 = 1$ atm are reference values for the temperature and the pressure. F is the mole fraction of burned gas diluent, T_u the temperature of the unburned gases, and α β and $S_{L,0}$ are functions that depend on the type of fuel and the fuel-to-air ratio. For gasoline they are

$$S_{L,0g} = 0.305 - 0.549(\phi - 1.21)^2 \quad (5.2)$$

$$\alpha_g = 2.4 - 0.271\phi^{3.51} \quad (5.3)$$

$$\beta_g = -0.357 + 0.14\phi^{2.77} \quad (5.4)$$

The first step was to calculate the sensitivity of the laminar burning speed to the different variables in the formula to see if it would be possible to separate changes in the EGR rate from errors in the other variables.

5.2 Sensitivity

The sensitivity is a measure of how much a change in a variable will affect the result of the calculation. The sensitivity is calculated like

$$S_a^y = \frac{dy}{da} \frac{a}{y} \quad (5.5)$$

where $y = f(a)$. In this case y is S_L of equation 5.1 and a is the different variables. For λ this gives

$$S_\lambda^{S_L} = \left[\frac{2(\lambda^{-1}-1.21)}{0.556-(\lambda^{-1}-1.21)^2} + 0.951\lambda^{-2.51} \ln \left(\frac{T_u}{T_0} \right) - 0.388\lambda^{-1.77} \ln \left(\frac{p}{p_0} \right) \right] \lambda^{-1} \quad (5.6)$$

The complete derivation of this equation can be found in appendix A. For the EGR rate the sensitivity is calculated like

$$S_{EGR}^{S_L} = -\frac{1.5862F^{0.77}}{1 - 2.06F^{0.77}} \quad (5.7)$$

The sensitivity towards errors in the temperature and pressure is equal to the values of α and β so

$$S_T^{S_L} = \alpha_g = 2.129 \quad (\lambda = 1) \quad (5.8)$$

$$S_p^{S_L} = \beta_g = -0.217 \quad (\lambda = 1) \quad (5.9)$$

As can be seen in the formulas above, the sensitivity to the pressure is very low and should not cause any problem. The sensitivity towards the temperature is high but this is not a big problem because the temperature of the inlet air is known and then the temperature at the ignition point can be calculated. To do this you need to know the cylinder geometry and assume an adiabatic compression. The temperature at a certain crank angle can then be calculated using

$$T_\theta = \left(\frac{V_{max}}{V_\theta} \right)^{\gamma-1} T_{in} \quad (5.10)$$

where V_θ is calculated like

$$V_\theta = V_{min} + \frac{\pi B^2}{4} \left(l + a - a \cos \theta + \sqrt{l^2 - a^2 \sin^2 \theta} \right) \quad (5.11)$$

The cylinder geometry is defined by, B the cylinder bore, l the length of the connecting rod, a the crank radius and V_{min} the free volume in the cylinder when the piston is at top dead center.

The pressure can also be calculated using the pressure in the inlet manifold and the same assumption, but as the pressure change is very small around the used ignition points and the sensitivity is low this can be neglected and instead one fixed value used.

In figure 5.1 The sensitivity of the laminar burning speed towards λ and EGR is plotted. From this figure you can see that around the assumed λ value of 1 the sensitivity is more or less 1 which means that if the assumed λ value is 2% wrong the calculated burning speed will also be wrong by 2%. This sensitivity value towards λ is within the acceptable limits, the effect from an incorrect λ value is not too big although a lower value would be preferred.

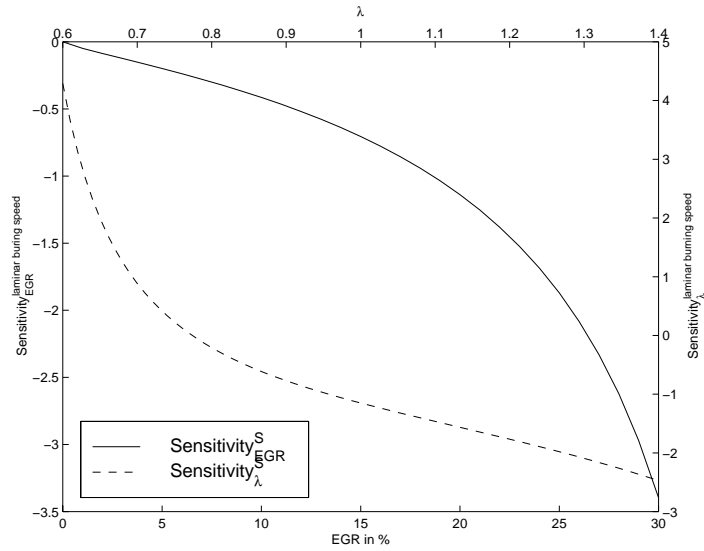


Figure 5.1: Sensitivity of the laminar burning speed to λ and EGR rate.

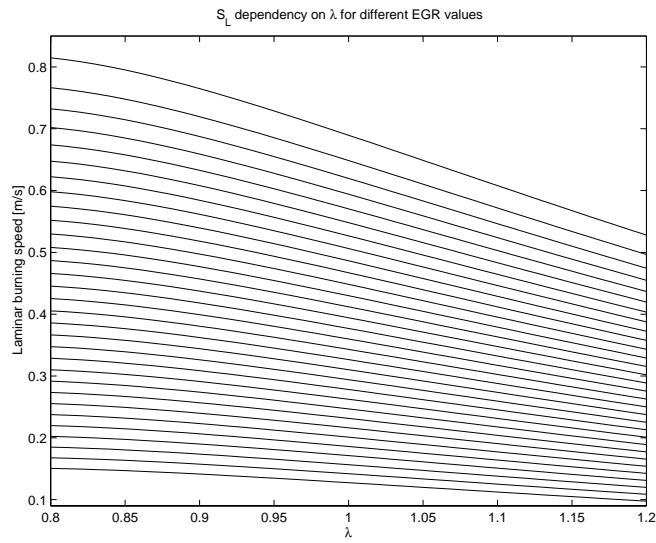


Figure 5.2: Effects on the laminar burning speed of different EGR rates and λ values.

For EGR it can be seen that the sensitivity to low rates is low but for higher EGR rates it is high. This is good as we want changes in the EGR rate to affect the burning speed strongly so that the changes can easily be detected. The high sensitivity towards EGR for high EGR rates should give a good possibility of separating the influence of the EGR on the laminar burning speed from the influence of the other variables.

Figure 5.2 shows the laminar burning speed as a function of λ . One line has been plotted for each EGR rate between 0 and 30%. For high EGR rates, at the bottom of the plot, it can be seen that the burning speed is almost constant in an area around $\lambda = 1$. This means that the influence of the EGR rate dominates over the influence from the air/fuel mixture.

The conclusion from these calculations is that there is a good chance of calculating the EGR rate correctly if the burning speed is known. The next step is to find a connection between the ionization signal and the laminar burning speed of the flame.

5.3 Flame kernel radius

To find a connection between the ion current signal and the flame speed the flame kernel radius was studied. The idea was that if the radius as a function of time could be plotted versus the ion current maybe some relationships could be seen. One possible relationship that should be tested is that the first maximum always occurs at a certain radius.

From [17] the following model of the flame kernel development was taken

$$\frac{dr_k}{dt} = \frac{\rho_u}{\rho_K} (S_t + S_{plasma}) + \frac{V_K}{A_K} \left[\frac{1}{T_K} \frac{dT_K}{dt} - \frac{1}{p} \frac{dp}{dt} \right] \quad (5.12)$$

in this formula the turbulent burning speed S_t can be calculated like

$$\begin{aligned} \frac{S_t}{S_l} = I_0 + I_0^{1/2} & \left(\frac{[\bar{U}^2 + u'^2]^{1/2}}{[\bar{U}^2 + u'^2]^{1/2} + S_l} \right)^{1/2} * \left(1 - e^{(-\frac{r_K}{L})} \right)^{1/2} * \\ & \left(1 - e^{-\frac{[\bar{U}^2 + u'^2]^{1/2} + S_l}{L} t} \right)^{1/2} * \left(\frac{u'}{S_l} \right)^{5/6} \end{aligned} \quad (5.13)$$

Due to lack of data over the engine some assumptions have to be made. In the formula for the turbulent burning speed the strain factor I_0 is assumed to be 1 which is approximately true. Due to the combustion system the mean flow velocity in the cylinder should be small and thus the assumption

is that \bar{U} is zero. This gives us the following equation for the turbulent burning speed.

$$S_t = S_l + \frac{S_l^{1/6} u'^{4/3}}{(u' + S_l)^{1/2}} \left(1 - e^{-\frac{r_K}{L}}\right)^{1/2} \left(1 - e^{-\frac{u' + S_l t}{L}}\right)^{1/2} \quad (5.14)$$

This leaves two unknown variables, the turbulence intensity u' and the integral length scale L . For the turbulence intensity the approximation made is that it is equal to 50% of the mean piston velocity

$$u' = 0.5\bar{v}_p = 0.5 \frac{120l}{rpm} \quad (5.15)$$

For the integral length scale L a value from another engine was used, but this value should be close to the true value.

In the model, equation 5.12, there are also some simplifications done. Both the pressure p and the temperature of the burned gases T_K should be almost constant during the early stages of the kernel. This means that the second term of equation 5.12 can be neglected. The term S_{plasma} includes the effect the ignition system has on the early flame kernel. These effects only affect the kernel for the very short time in the beginning of the combustion when the flame is still attached to the electrodes of the spark plug. By setting the initial conditions for the radius calculations to after this time the term S_{plasma} can also be neglected. This leaves us with the following formula for the speed with which the flame kernel propagates through the cylinder.

$$\frac{dr}{dt} = \frac{\rho_u}{\rho_K} \left(S_l + \frac{S_l^{1/6} u'^{4/3}}{(u' + S_l)^{1/2}} \left(1 - e^{-\frac{r_K}{L}}\right)^{1/2} \left(1 - e^{-\frac{u' + S_l t}{L}}\right)^{1/2} \right) \quad (5.16)$$

The densities, ρ , for the air and the fuel are taken from tables. The values in the tables are for reference conditions and they need to be recalculated to accommodate the higher temperatures in the engine. This can be done by using

$$\rho_2 = \rho_1 \frac{T_1}{T_2} \quad (5.17)$$

The density for the unburned gases ρ_u are calculated in the following way

$$\rho_u = (1 - F) (14.3\rho_{air} + \rho_{fuel}) \frac{273}{T_{in}} + F\rho_{EGR} \quad (5.18)$$

In this equation a λ value of 1 is assumed. The density of the exhaust gas are given by

$$\rho_{exhaust} = \frac{m}{V} = \frac{p}{RT} = \frac{p_{exhaust}}{RT_{exhaust}} \quad (5.19)$$

giving the final formula for the density of the unburned gases when the density of the burned gases are updated according to equation 5.17 and assuming that the pressure in the exhaust pipe is 1 atm

$$\rho_u = (1 - F) (14.3\rho_{air} + \rho_{fuel}) \frac{273}{T_{in}} + \frac{F}{RT_{in}} \quad (5.20)$$

For the kernel density ρ_K equation 5.19 is used but with data for the flame kernel giving

$$\rho_K = \frac{p_K}{R_K T_K} \quad (5.21)$$

Equations 5.1-5.4, 5.14-5.16 and 5.20-5.21 now give our complete model over the speed with which the flame kernel propagates through the cylinder.

Using the model a calculation of the flame radius as a function of time was made. The calculation of the radius first updates the three different speeds, laminar flame speed, turbulent flame speed and the speed with which the kernel grows for each time step. Here the laminar burning speed is needed to get the turbulent burning speed which in turn is needed to get the kernel speed. The next step is to calculate the new radius, this is done by updating the previous radius with the kernel speed times the time step using

$$r_K^+ = r_K^- + \frac{dr_K}{dt} \Delta t \quad (5.22)$$

For each EGR rate between 0% and 25% in steps of 5% the calculations was done for 500 time steps. The calculated radius for each EGR rate was then plotted versus the ion current signal of that EGR rate, the plots can be seen in figure 5.3. As can be seen in the figure no direct connection between the ion current signal and the kernel radius can be found.

The idea that the flame kernel radius always should be the same at the position for the first maximum is not valid. It can be seen in figure 5.3 but it is made clearer in figure 5.4. In this figure the radius at the time of the peak of the first maximum and the position of this peak are plotted for different EGR rates. In the figure it can be clearly seen that the radius do not have the same value for the different peak positions.

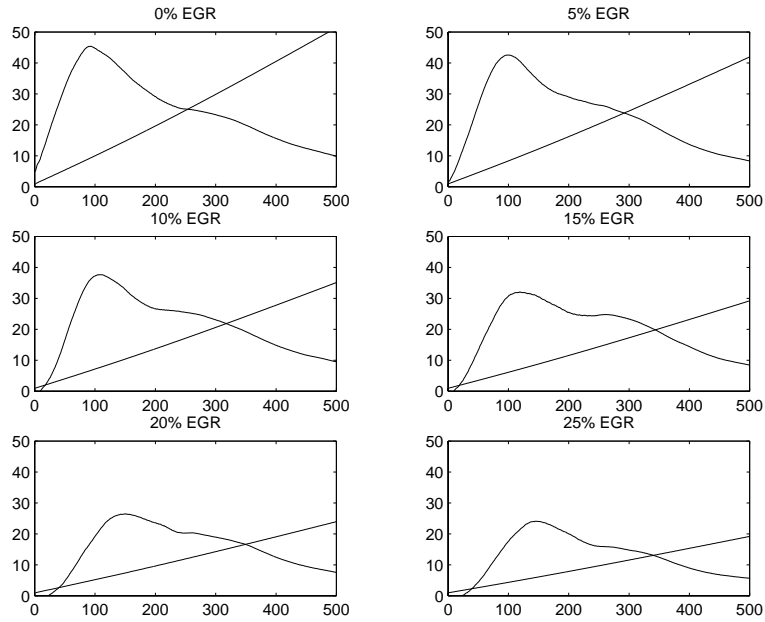


Figure 5.3: The flame kernel radius and the ion current signal plotted for different EGR rates.

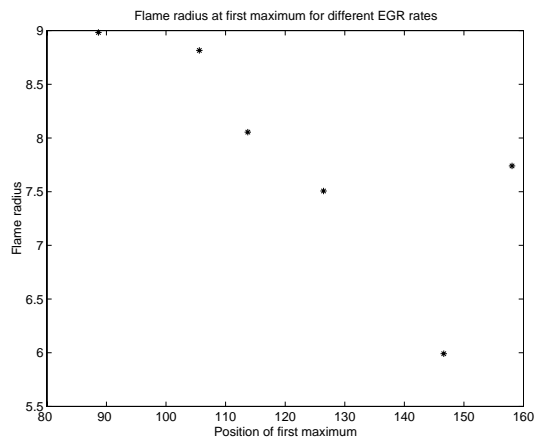


Figure 5.4: The kernel radius at the position of the first maximum for different EGR rates.

5.4 EGR estimation

As no physically based formula for calculating the flame speed directly from the ion current signal could be found in the previous section, no good way of estimating the EGR through the laminar burning speed was created. If the flame speed is to be used then fitting is required to take the step from ion current to flame speed. To first do the fitting to the flame speed and then from the flame speed calculate the EGR rate has no benefits over fitting the ion current directly to the EGR rate like it is done in the section 4.1.

To get the flame speed from the ion current a few different ways might be possible. One idea is to look closer at the reaction kinetics and thermodynamics of the combustion process to try to get a good model of how the flame speed or the kernel radius affects the ion current.

Another idea is that in engines with two spark plugs during some cycles only one spark plug would be used for igniting the mixture and then the other spark plug is used to measure. Thus knowing the distance between the spark plugs and the time between the ignition and when the flame front reaches the second spark plug the flame speed could be calculated. This method could not be tested since the engine used for this thesis only has one spark plug.

6 Conclusions

The ionization signal from the GDI engine working in stratified mode differs from the signal from an engine with homogeneous mixture in the way that there is no clearly visible second maximum of the signal.

The introduction of external EGR in the cylinder affects the ion current signal in different ways. In the flame-front phase the amplitude of the first maximum is lowered and it occurs later. The area under the maximum, representing the total amount of ions in this phase, is decreased. For the post-flame phase the two effects of lower amounts of NO_x and less excess air in the cylinder balance each other. This means that no information about the EGR rate can be found from this part of the signal and that the flame-front phase of the signal must be used.

Of the two algorithms for estimating the EGR rate that are based on the general knowledge of how the amount of EGR affects the ion current signal the algorithm with the static Kalman filter gave the best result. With this filter an accurate result could be obtained within 40 cycles. Another benefit with this filter is that the computational resources needed is low. The troubles with the static filter is that it is a bit slow and that the filter has to be reset to be able to estimate a new EGR rate.

The second algorithm that uses the dynamical Kalman filter showed that these two effects can not be corrected at the moment. If a faster response time is wanted and the need for resetting the filter is removed the output never stabilizes, it reaches approximately the right value but oscillates around it.

The formula for the laminar burning speed of the flame would prove a good way for calculating the EGR rate if a physically based connection between the flame speed and the ion current signal could be found. Unfortunately no such connection could be found.

References

- [1] H. Johansson J. Auzins and J. Nytomt. Ion-gap sense in missfire detection, knock and engine control. *SAE paper No. 950004*, 1995.
- [2] Lars Eriksson. *Spark Advance Modeling and Control*. PhD thesis, Linköpings University, 1999.
- [3] Lars Eriksson, Lars Nielsen, and Mikael Glavenius. Closed loop ignition control by ionization current interpretation. *SAE paper No. 970854*, 1997.
- [4] Lars Nielsen and Lars Eriksson. An ion-sense engine-fine-tuner. *IEEE control systems (special issue on powertrain control)*, Vol. 18(5):43–52, October 1998.
- [5] E. N. Balles, A. VanDyne, A. M.Wahl, K. Ratton and M. C. Lai. In-Cylinder Air/Fuel Ratio Approximation Using Spark Gap Ionization Sensing. *SAE paper No. 980166*, 1998.
- [6] John B. Heywood. *Internal Combustion Engine Fundamentals*. Automotive Technology Series. McGraw-Hill, 1988.
- [7] Helmut Eichseder, Eckard Baumann, Peter Müller and Stephan Rubbert. Gasoline Direct Injection - A Promising Engine Concept for Future Demands. *SAE paper No. 2000-01-0248*, 2000.
- [8] Michihiko Tabata, Toshihide Yamamoto and Tugio Fukube. Improving NO_x and Fuel Economy for Mixture Injected SI Engine with EGR. *SAE paper No. 950648*, 1995.
- [9] H. Wilstermann, A. Greiner, P. Hohner, R. Kremmlerm, R.R Maly and J. Schenk. Ignition system integrated AC ion current sensing for robust and reliable online engine control. *SAE paper No. 2000-01-0553*, 2000.
- [10] Reymond Reinmann. *Theoretical and Experimental Studies of the Formation of Ionized Gases in Spark Ignition Engines*. PhD thesis, Lund Institute of Technology, 1998.
- [11] H.F.Calcote. Mechanisms for the formation of ions in flames. *Combustion and Flames*, Volume 1:385–403, 1957.
- [12] H.F.Calcote. Ion production and recombination in flames. *Eight (International) Symposium on combustion*, page 184, 1962.

-
- [13] André Saitzkoff, Raymond Reinmann and Fabian Mauss. In-Cylinder Pressure Measurements Using the Spark Plug as an Ionization Sensor. *SAE paper No. 970857*, 1997.
 - [14] Peter S. Maybeck. *Stochastic models, estimation and control*, volume 1. Academic Press, 1979.
 - [15] Eva Finkeldei. *Auswertung des Ionenstromsignals zur Bestimmung des Kraftstoff-Luft-Verhältnisses und der Abgasrückführrate am OttoDE*. Diplomarbeit, Fachhochschule Aachen, 1999.
 - [16] Christian Sixel. Entwurf von digitalen filtern zur filterung des ionenstromsignals beim direkteinspritzenden ottomotor. Praktikumsbericht, Fachhochschule Trier, 2000.
 - [17] R. Herweg and R. R. Maly. A fundamental model for flame kernel formation in S.I. engines. *SAE paper No. 922243*, 1992.

Appendix A: Derivation of the sensitivity formula $S_\lambda^{S_L}$

Here are the complete calculations presented that leads to the final equation 5.6 for the sensitivity of the laminar burning speed to λ .

Using equation 5.5 to calculate the sensitivity of S_L to λ we get

$$S_\lambda^{S_L} = \frac{dS_L}{d\lambda} \frac{\lambda}{S_L} \quad (\text{A.1})$$

inserting equation 5.1 into A.1 gives

$$S_\lambda^{S_L} = \frac{d\left(S_{L,0}(\lambda) \left(\frac{T_u}{T_0}\right)^{\alpha(\lambda)} \left(\frac{p}{p_0}\right)^{\beta(\lambda)} (1-2.06F^{0.77})\right)}{d\lambda} \frac{\lambda}{S_{L,0}(\lambda) \left(\frac{T_u}{T_0}\right)^{\alpha(\lambda)} \left(\frac{p}{p_0}\right)^{\beta(\lambda)} (1-2.06F^{0.77})} \quad (\text{A.2})$$

using the general rule of how to derivate products we have

$$\begin{aligned} \frac{dS_L}{d\lambda} &= \frac{dS_{L,0}(\lambda)}{d\lambda} \left(\frac{T_u}{T_0}\right)^{\alpha(\lambda)} \left(\frac{p}{p_0}\right)^{\beta(\lambda)} (1-2.06F^{0.77}) + \\ &\frac{d\left(\left[\frac{T_u}{T_0}\right]^{\alpha(\lambda)}\right)}{d\lambda} S_{L,0}(\lambda) \left(\frac{p}{p_0}\right)^{\beta(\lambda)} (1-2.06F^{0.77}) + \\ &\frac{d\left(\left[\frac{p}{p_0}\right]^{\beta(\lambda)}\right)}{d\lambda} S_{L,0}(\lambda) \left(\frac{T_u}{T_0}\right)^{\alpha(\lambda)} (1-2.06F^{0.77}) \end{aligned} \quad (\text{A.3})$$

to derivate the exponents like $A^{f(\lambda)}$ we first rewrite the function

$$y(x) = A^{f(x)} = e^{\ln(A^{f(x)})} = e^{f(x)\ln(A)} = e^{g(x)} \quad (\text{A.4})$$

now the normal rules for derivating an exponential function can be used to give

$$\begin{aligned} \frac{dy(x)}{dx} &= g'(x) e^{g(x)} = f'(x) \ln(A) e^{f(x)\ln(A)} \\ &= f'(x) \ln(A) e^{\ln(A^{f(x)})} = f'(x) \ln(A) A^{f(x)} \end{aligned} \quad (\text{A.5})$$

using A.5 on A.3 yields

$$\begin{aligned} \frac{dS_L}{d\lambda} &= \left(\left(\frac{T_u}{T_0}\right)^\alpha \left(\frac{p}{p_0}\right)^\beta (1-2.06F^{0.77}) \right) \\ &\left(\frac{dS_{L,0}}{d\lambda} + S_{L,0} \frac{d\alpha}{d\lambda} \ln\left(\frac{T_u}{T_0}\right) + S_{L,0} \frac{d\beta}{d\lambda} \ln\left(\frac{p}{p_0}\right) \right) \end{aligned} \quad (\text{A.6})$$

inserting equation A.6 into equation A.2 with simplification of the term $\left(\left(\frac{T_u}{T_0}\right)^\alpha \left(\frac{p}{p_0}\right)^\beta (1 - 2.06F^{0.77})\right)$ gives

$$S_\lambda^{S_L} = \left(\frac{dS_{L,0}}{d\lambda} + S_{L,0} \frac{d\alpha}{d\lambda} \ln \left(\frac{T_u}{T_0} \right) + S_{L,0} \frac{d\beta}{d\lambda} \ln \left(\frac{p}{p_0} \right) \right) \frac{\lambda}{S_{L,0}} \quad (\text{A.7})$$

Next comes the derivations of equations 5.2-5.4, with $\phi = \lambda^{-1}$ we have

$$\frac{dS_{L,0}}{d\lambda} = 1.098 (\lambda^{-1} - 1.21) \lambda^{-2} \quad (\text{A.8})$$

$$\frac{d\alpha}{d\lambda} = 0.951 \lambda^{-4.51} \quad (\text{A.9})$$

$$\frac{d\beta}{d\lambda} = -0.388 \lambda^{-3.77} \quad (\text{A.10})$$

equations A.8-A.10 inserted into A.7 gives

$$S_\lambda^{S_L} = \frac{1.098(\lambda^{-1}-1.21)\lambda^{-2}}{0.305-0.549(\lambda^{-1}-1.21)^2} \lambda + 0.951\lambda^{-4.51} \ln \left(\frac{T_u}{T_0} \right) \lambda - 0.388\lambda^{-3.77} \ln \left(\frac{p}{p_0} \right) \lambda \quad (\text{A.11})$$

in the first term the value of $S_{L,0}$ from equation 5.2 has been inserted and in the last two terms this factor has been simplified. Some small changes yields the final result

$$S_\lambda^{S_L} = \left[\frac{2(\lambda^{-1}-1.21)}{0.556-(\lambda^{-1}-1.21)^2} + 0.951\lambda^{-2.51} \ln \left(\frac{T_u}{T_0} \right) - 0.388\lambda^{-1.77} \ln \left(\frac{p}{p_0} \right) \right] \lambda^{-1} \quad (\text{A.12})$$

which is equation 5.6.